

LETTER TO THE JOURNAL

Sexual dimorphism in the antitumor immune responses elicited by the combination of fasting and chemotherapy

Fasting reduces chemotherapy toxicity [1], enhances immunogenic tumor cell death [2, 3] and increases CD8⁺ T cell infiltration in tumors, particularly when combined with chemotherapy [2, 3] or immunotherapy [4]. Moreover, fasting exhibits a sexual dimorphism in the immune system [5].

The aim of our study was to elucidate the role of sex in the beneficial anti-tumoral effects of combining fasting and chemotherapy. For this, we inoculated B16-F10-derived melanoma allografts into immunocompetent male and female mice. Three days later, the mice were divided into: (1) not treated; (2) two cycles of 48-hour fasting; (3) two cycles of 10 mg/kg doxorubicin; (4) two cycles of doxorubicin and fasting for 24 hours before and 24 hours after doxorubicin inoculation (“combination treatment” or “CT”). The study methods are shown in the Supplementary Material file. Doxorubicin and fasting alone reduced tumor growth in both sexes with the same efficacy, and CT amplified this effect only in males (Figure 1A and Supplementary Figure S1A-C). Male mice bearing YUMM1.7 melanoma-derived tumors responded to fasting and doxorubicin, but females were insensitive to any of them (Figure 1B and Supplementary Figure S2A-C). Oxaliplatin did not affect B16-F10 tumor growth (Supplementary Figure S3A-D). Fasting reduced serum levels of testosterone only in males ([6, 7] and Supplementary Figure S4A). To explore the role of testosterone, we castrated males or implanted testosterone pellets in females. CT lost efficacy in castrated males and became

efficient in females with testosterone pellets (Figure 1C and Supplementary Figure S4B-E). Next, we inoculated mice with MC38 colon carcinoma cells [8]. Oxaliplatin or fasting reduced tumor growth, and CT amplified this effect in both sexes (Figure 1D and Supplementary Figure S5A-C). Our findings indicate that sexual dimorphism occurs in different tumor types, is dependent on tumor and chemotherapy type, and testosterone is a key player in this sexual dimorphism.

To study the immune response in B16-F10 allografts treated with doxorubicin and/or fasting (Supplementary Figure S6A-D), we analyzed relevant immune cell types in inguinal lymph nodes (LN), peripheral blood (B) and tumors (T) (Supplementary Table S1-S4). CT increased stage II Natural Killer (NK) and Natural Killer T (NKT) cells in B16-F10 tumors only in males (Figure 1E-F and Supplementary Figure S6E-H). Females on CT had more exhausted CD8⁺ T cells in their tumors (Figure 1G and Supplementary Figure S6I-K). Tumor-infiltrated CD8⁺ T cells were functionally more active in CT in males (Supplementary Figure S7A-C), while serum TNF α did not change (Supplementary Figure S7D-E). Immunoablation of CD8 cells in male mice tended to reduce CT efficacy, which still improved the antitumor response (Supplementary Figure S8A-F and Supplementary Table S5), indicating that immune cell populations other than CD8 cells were also involved in this response. Evolution with treatment and sex of all other analyzed populations is shown in Supplementary Figure S9A-L and S10A-J. The transcription of many cytokines and chemokines was strongly upregulated in CT only in males (Supplementary Figure S11A-B). Finally, we treated male and female Hsd:Athymic Nude-Foxn1^{nu} mice lacking T lymphocytes with the same protocol. Fasting alone did not reduce tumor progression; single chemotherapy reduced tumor growth, and CT enhanced chemotherapy efficacy mostly in male mice (Supplementary Figure S12A-H). These results suggest that the beneficial effects of CT are dependent on the cellular immune system, particularly on NK and NKT cells. We then performed a high-dimensional

Abbreviations: B, peripheral blood; CD, cluster of differentiation; CT, combination treatment; Foxn1, forkhead box N1 gene; Hsd, Harlan Sprague Dawley; LN, lymph nodes; MDSC, myeloid-derived suppressor cells; M-MDSC, monocytic myeloid-derived suppressor cells; NK, natural killer cells; NKT, natural killer T cells; nu, nude; pDC, plasmacytoid dendritic cells; PD-1, programmed cell death protein 1; PMN-MDSC, polymorphonuclear myeloid-derived suppressor cells; T, tumors; Th1, T helper type 1; TIM-3, T-cell immunoglobulin mucin-3; YUMM, Yale University Mouse Melanoma.

Manuel Montero and Jose Ignacio Escrig contributed equally as second authors.

This is an open access article under the terms of the [Creative Commons Attribution-NonCommercial-NoDerivs](https://creativecommons.org/licenses/by-nc-nd/4.0/) License, which permits use and distribution in any medium, provided the original work is properly cited, the use is non-commercial and no modifications or adaptations are made.

© 2024 The Authors. *Cancer Communications* published by John Wiley & Sons Australia, Ltd. on behalf of Sun Yat-sen University Cancer Center.

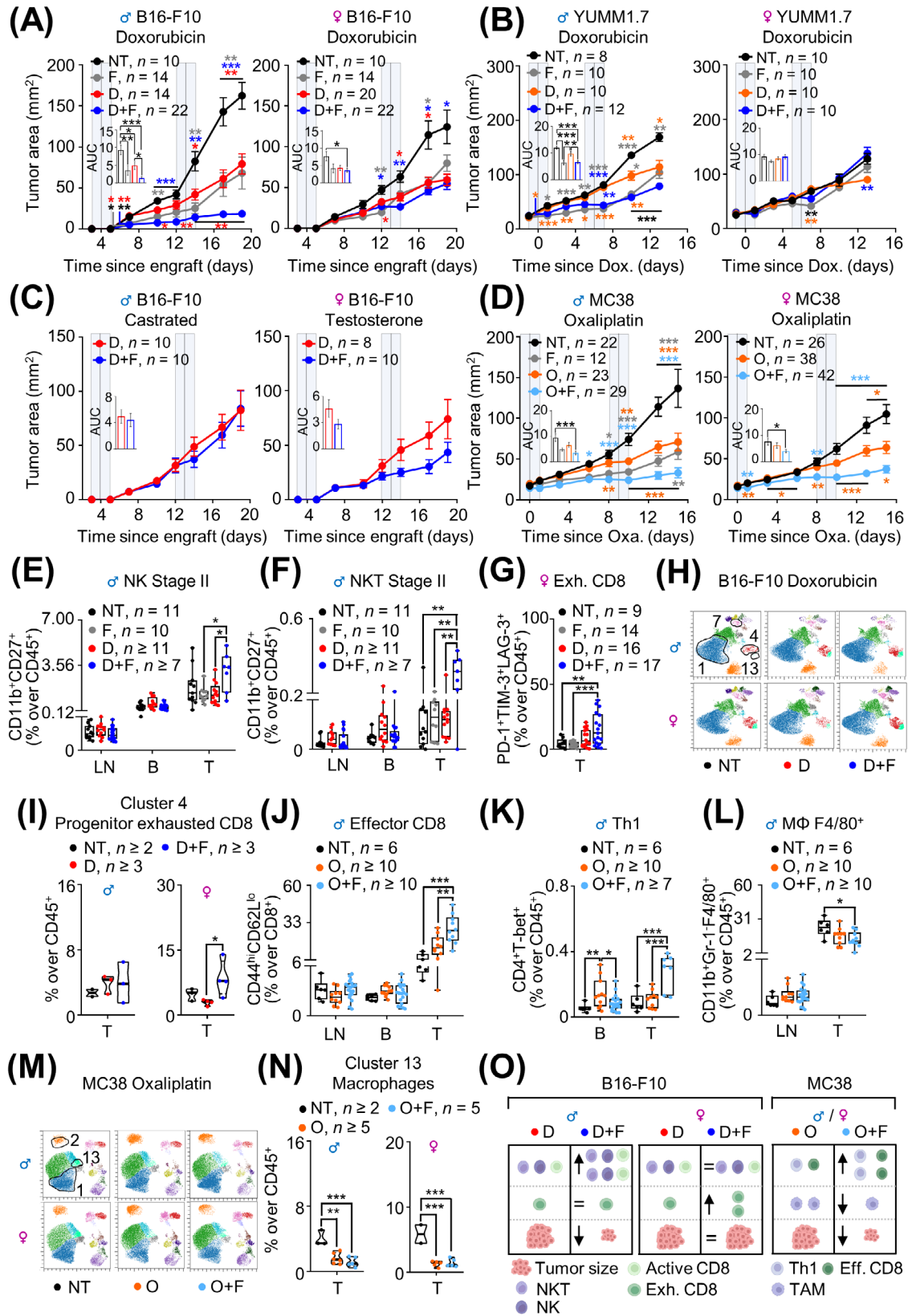


FIGURE 1 Sexual dimorphism in the antitumor immune responses elicited by the combination of fasting and chemotherapy. (A) Male and female 12-22-week-old mice were inoculated subcutaneously with melanoma B16-F10 cells. Some mice were left untreated (NT group); fasted for 2 cycles of 48 hours (F group); inoculated intraperitoneally with two cycles of 10 mg/kg doxorubicin 4 and 13 days after the inoculation of B16-F10 cells and fed with a standard diet (D group, indicated by vertical grey lines); or inoculated with 10 mg/kg doxorubicin and followed a 48-hour fast around each chemotherapy cycle (D+F group, indicated by grey boxes). Tumor progression was monitored on the

analysis of the immune populations in the tumors using 17 surface markers representing relevant immune populations (Supplementary Table S6). After a dimensional reduction and unsupervised clustering, we obtained 13 immune clusters (Figure 1H and Supplementary Figure S13A) and quantified the differential presence of these immune cell types between experimental groups (Supplementary Figure S13B). Cluster 1 (M2 macrophages) was increased in chemotherapy and CT only in males (Supplementary Figure S13C), coinciding with Supplementary Figure S10J. Clusters 4 and 13, expressing markers of exhaustion (TIM-3 and PD-1), tended to be higher in females on CT (Figure 1I and Supplementary Figure S13D), confirming Figure 1G. Cluster 7 (stage I NKT) was significantly increased in CT compared with chemotherapy

alone in both sexes (Supplementary Figure S13E). Next, we focused on CD8⁺ T cells (Supplementary Figure S14A-B). Cluster 14 (exhausted central memory/effector CD8 cells) was increased following CT in both sexes (Supplementary Figure S14C-D). Clusters 18 and 20 (regulatory CD8 T cells [9]) tended to be decreased only in males with chemotherapy alone (Supplementary Figure S14C and E). These findings stress the differential response of CD8 cells between both sexes to chemotherapy and CTs. We also checked for sub-clusters within the NK1.1⁺ cells and did not find informative sub-clusters (Supplementary Figures S14F-G).

We then analyzed the immune populations in mice bearing MC38 colon carcinoma cells (Figure 1D). CT increased total intratumoral effector and exhausted CD8⁺

indicated days after the inoculation of the tumor cells and the tumor area in mm² is represented. The area under the curve (AUC) is shown as an inset in each panel. (B) Male and female 11-22-week-old mice were inoculated subcutaneously with the YUMM1.7 cell line. Tumors grew until they reached a 13-47 mm² tumor area, having 25 mm² as the average size. Then, the chemotherapy and/or fasting treatments began as indicated by the grey boxes. Treatment groups were the same as indicated in (A). Tumor progression was monitored on the indicated days from the day before chemotherapy injection and the tumor area in mm² is represented. The area under the curve (AUC) is shown as an inset in each panel. (C) Male mice were castrated at 8 weeks of age, and B16-F10 cells were inoculated subcutaneously 7-9 weeks later. 25 mg testosterone was implanted subcutaneously in pellets to 12-16-week-old female mice, and 11 days later B16-F10 cells were inoculated subcutaneously. After tumor implantation, treatment groups (D and D+F) are the same as those described in (A). Tumor progression was monitored on the indicated days after the inoculation of the tumor cells. The area under the curve (AUC) is shown as an inset in each panel. (D) Male and female 11-19-week-old mice were inoculated subcutaneously with the colon carcinoma cell line MC38. Tumors grew until they reached a 5-38 mm² tumor area, having 16 mm² as the average size. Then, the chemotherapy and/or fasting treatments began as indicated by the grey boxes. Some mice were left untreated (NT group); fasted for 2 cycles of 48 hours (F group); were inoculated intraperitoneally with two cycles of 7.5 mg/kg oxaliplatin at the indicated days after tumors reached the initial size and were fed with a standard diet (O, indicated by vertical grey lines); or were inoculated with 7.5 mg/kg oxaliplatin and followed a 48-hour fast around each chemotherapy cycle (O+F group, indicated by grey boxes). Tumor progression was monitored on the indicated days after the first chemotherapy inoculation and the tumor area in mm² is represented. The area under the curve (AUC) is shown as an inset in each panel. (E-G) Tumor-draining lymph nodes (LN), peripheral blood (B) and B16-F10 tumor (T) samples obtained from mice shown in Supplementary Figure 6A-D six days after the second chemotherapy cycle were analyzed by flow cytometry (Supplementary Tables 1-4) for the indicated immune populations: NK Stage II, NKT Stage II and exhausted CD8 cells. (H) B16-F10 allograft samples from a group of male and female mice treated as in (A) were obtained six days after the second doxorubicin cycle, and the intra-tumoral immune response was analyzed using a panel of 17 surface markers (Supplementary Table S6). After dimensional reduction and clustering, a set of 13 clusters was identified in every treatment group, according to the marker expression shown in Supplementary Figure 13A. The color code of the dot plots is represented on Supplementary Figure 13A. Populations that changed significantly between different conditions are circled. (I) Quantification of cells in Cluster 4 (circled in the dot plot in H) in the tumor of mice under the indicated treatments. (J-L) Quantification of the indicated immune populations in tumor samples from mice shown in (D). (M) MC38 allograft samples from a group of male and female mice treated as in (D) were obtained six days after the second oxaliplatin cycle, and the intra-tumoral immune response was analyzed using a panel of 19 surface markers (Supplementary Table S7). After dimensional reduction and clustering, a set of 15 clusters was identified in every treatment group, according to the marker expression shown in Supplementary Figure 21A. The color code of the dot plots is represented in Supplementary Figure 21A. (N) Quantification of cells in Cluster 13 (marked in the dot plot in M) in the tumor of mice under the indicated treatments. (O) The diagram summarizes the observations in the B16-F10 and MC38 tumor models. The gating strategy used for the immune populations of the classical cytometry is indicated in Supplementary Tables S1-4 or cell discrimination for the high-dimensional cytometry was made according to each marker expression as indicated in Supplementary Figure S13A and S21A. Line-connected dots and bars represent the average of the indicated number of tumors. Error bars represent the standard error of the mean. Statistical significance was assessed with the two-tailed unpaired t-test (insets in C); with the one-way ANOVA test (E-G, I-L, N; insets in A-B, D); with the two-way ANOVA with mixed effects model (line graphs, A-D). In the ANOVA analysis, Tukey's (A-B, D) or Sidak's (C) correction for multiple comparisons was used. *, *P* < 0.05; **, *P* < 0.01; ***, *P* < 0.001. Colors of asterisks placed next to data points indicate the treatment group to which that point is significantly different. Abbreviations: AUC: area under the curve; B: peripheral blood; CD: cluster of differentiation; D: doxorubicin; Dox.: doxorubicin; Eff.: effector; Exh.: exhausted; F: fasting; LAG-3: lymphocyte activation gene 3; LN: lymph nodes; MΦ: macrophages; NK: natural killer cells; NKT: natural killer T cells; NT: not treated; O: oxaliplatin; Oxa.: oxaliplatin; PD-1: programmed cell death protein 1; T: tumor; TAM: tumor-associated macrophages; TIM-3: T cell immunoglobulin domain and mucin domain 3; Th1: T helper type 1; YUMM: yale university mouse melanoma.

cells (Figure 1J and Supplementary Figure S15A-D). CD8 tumor infiltration was more active in fasting, chemotherapy and in CT than in the untreated mice (Supplementary Figure S15E-F). CT also increased intratumoral CD4 Th1 cells, with anti-tumoral properties (Figure 1K and Supplementary Figure S16A). Total intratumoral macrophages, with pro-tumoral properties, were decreased with CT (Figure 1L and Supplementary Figure S16B). The evolution of all other analyzed populations in both sexes is shown in Supplementary Figures S17-19, where populations in females behaved very similarly to males. Tumor cytokine and chemokine transcription did not significantly change with treatment or sex (Supplementary Figure S20A-B). High-dimensional analysis of the intratumoral immune populations using 19 surface markers (Supplementary Table S7), followed by a dimensional reduction and unsupervised clustering, generated 15 clusters (Figure 1M and Supplementary Figure S21A). Cluster 1 (M-MDSC) was reduced with chemotherapy and CT (Supplementary Figure S21B-C); Cluster 2 (PMN-MDSC) was increased in CT, especially in males (Supplementary Figure S21B and D); and Cluster 13 (tumor-associated macrophages) was reduced in both treatments and sexes (Figure 1N and Supplementary Figure S21B). The evolution of these three populations fit with our previous results (Figure 1L and Supplementary Figure S18I-L and S19C).

We analyzed tumor-draining lymph nodes and blood for a physiological understanding of the immune response. CT increased lymph node MDSC only in females bearing B16-F10 (Supplementary Figure S10B), partly explaining the failure of females to respond to fasting, and this change was not reflected in the tumors (Supplementary Figure S10A). CT increased lymph node-relevant central memory and naïve CD8 cells in the B16-F10 model in both sexes (Supplementary Figure S9C-D), and this was not reflected in blood or tumors. NK and NKT cells were important in the B16-F10 model: in males, CT decreased NK cells in the blood and increased them in the tumor (Supplementary Figure S9E), while stage II NKT cells were only increased in the tumor (Figure 1F). Comparing both tumor models, doxorubicin reduced total immune cells in blood and lymph nodes but oxaliplatin did not (Supplementary Figures S9A and S17A). These results indicate different global responses of the immune system between tumor types and that changes in blood or lymph nodes did not reflect those observed in tumors, in contrast to previous reports [10].

Our work confirms the beneficial effects of combining fasting with chemotherapy (doxorubicin and oxaliplatin) in mice. We observe for the first time a sexual dimorphism in this process with relevant clinical implications. Finally, we show that different tumor models show distinct immune responses, and therefore, the chemotherapy-

enhancing ability of fasting may not depend on specific immune populations (Figure 1O).

AUTHOR CONTRIBUTIONS

Andrés Pastor-Fernández: conceptualization; experimental design and performance; writing manuscript. **Manuel Montero Gómez de las Heras and Jose Ignacio Escrig-Larena:** high-dimensional immune methodology; formal analysis and investigation. **Marta Barradas:** immunofluorescence study design and analysis. **Cristina Pantoja:** project administration; data acquisition and curation, and mouse sample processing. **Adrian Plaza:** mouse sample processing; investigation and data interpretation. **Jose Luis Lopez-Aceituno:** mouse sample processing and technique optimization. **Esther Durán:** sample processing for immunofluorescence studies. **Alejo Efeyan:** support with immunofluorescence experiments. **Maria Mittelbrunn:** support with high-dimensional cytometry experiments. **Lola Martinez:** support with classical cytometry experiments; Pablo Jose Fernandez-Marcos: conceptualization; experimental design; funding and manuscript writing.

ACKNOWLEDGMENTS

We express our sincere appreciation for the key contributions of many colleagues whose instrumental support has been crucial to the realization of this work. We thank Arantzazu Sierra Ramírez, Ildefonso Rodríguez Ramiro, Luis Filipe Costa Machado and colleagues at IMDEA Food for their invaluable technical assistance and scientific discussions in the project. We acknowledge Eladio Martínez, Iván Jarreño, Antonio Morales and Ángel Naranjo, for their support within the CNB animal facility. Additionally, we are thankful to Marisol Soengas (CNIO) for providing the B16-F10 and YUMM1.7 cell lines, as well as Elena Fueyo Marcos and Óscar Fernández Capetillo (CNIO) for their contribution of the MC38 cell line. We really appreciate the protocols shared about immunodepleting experiments by Raquel Blanco Fuentes (CNB), Elena Meléndez Esteban (IRB) and Manuel Serrano Marugán (IRB). Purificación Muñoz and Laura Lorenzo Sanz (IDIBELL) deserve our thanks for sharing their technical protocols related to immunofluorescence studies. We also acknowledge Patricia González García and the histopathology unit (CNIO) for their assistance in deparaffinization and antigen retrieval. Technical support for immunofluorescence panel design and analysis was provided by José Miguel Rodríguez Frade and Ricardo Villares (CNB). Likewise, we are grateful to Cristina Ramírez and Virginia Pardo Marqués (IMDEA Food) for their valuable technical assistance in immunofluorescence studies. The expertise of Carmen Sánchez Jiménez, Carlos Gallego García, and Álvaro Sahún Español greatly assisted us within the confocal unit

at CBMSO. Lastly, we kindly appreciate the scientific help with the testosterone regulation of Ferran Martínez García (UJI) and Carmen Agustín Pavon (UV).

CONFLICT OF INTEREST STATEMENT

The authors have declared that no conflict of interest exists.

FUNDING INFORMATION

Andrés Pastor Fernández was a recipient of a predoctoral fellowship from the Spanish Association Against Cancer – AECC (PRDMA18011PAST). Cristina Pantoja and Marta Barradas were funded by the Madrid Institute for Advanced Studies (IMDEA) Food. Adrián Plaza was funded by the AECC (SIRTBIO-LABAE18008FERN). Jose Luis Lopez-Aceituno was funded by the Spanish Ministry of Science and Innovation (MICINN) (PTA2017-14689-I). Pablo Jose Fernandez-Marcos was funded by a Ramon y Cajal Award from the Spanish Ministry of Science, Innovation and Universities (MICINN) (RYC-2017-22335 /AEI/10.13039/501100011033). Work at the laboratory of Pablo Jose Fernández-Marcos was funded by the AECC (SIRTBIO- LABAE18008FERN) and the RETOS Program projects from the MICINN (SAF2017-85766-R/AEI/10.13039/501100011033 and PID2020-114077RB-I00/AEI/10.13039/501100011033).

Work in Lola Martínez flow cytometry unit was funded by the CNIO. Manuel Montero Gómez de las Heras and Jose Ignacio Escrig-Larena were supported by FPU grants (FPU19/02576 and FPU20/04066, respectively) from the Spanish Ministry of Science, Innovation and Universities. Work in the laboratory of Maria Mittelbrunn was supported by the Fondo de Investigación Sanitaria del Instituto de Salud Carlos III (PI19/855), the European Regional Development Fund (ERDF) and the European Commission through H2020-EU.1.1, European Research Council grant ERC-2016-StG 715322-EndoMitTalk, and the Y2020/BIO-6350 NutriSION-CM synergy grant from Comunidad de Madrid. Esther Durán was funded by the Centro de Estudios Universitarios (CEU) San Pablo University. Alejo Efeyan is an EMBO Young Investigator. Alejo Efeyan lab is supported by the Retos Projects Program of the Spanish Ministry of Science, Innovation and Universities, the Spanish State Research Agency (AEI/10.13039/501100011033), co-funded by the European Regional Development Fund (PID 2019-104012RB-I00), a FER0 Grant for Research in Oncology, and La Caixa Foundation (HR21-00046).

DATA AVAILABILITY STATEMENT




The data that support the findings of this study are available from the corresponding author upon reasonable request.

ETHICS APPROVAL

All animal experiments were performed according to the protocols approved by the Spanish National Research Council (CSIC) Ethics Committee for Research and Animal Welfare in Spain and all the appropriate official entities (PROEX 148/18 and 249.3/20).

CONSENT FOR PUBLICATION

Not applicable.

Andrés Pastor-Fernández¹ 
 Manuel Montero Gómez de las Heras² 
 Jose Ignacio Escrig-Larena²
 Marta Barradas¹
 Cristina Pantoja¹
 Adrian Plaza¹
 Jose Luis Lopez-Aceituno¹
 Esther Durán^{1,3}
 Alejo Efeyan⁴
 Maria Mittelbrunn²
 Lola Martínez⁵
 Pablo Jose Fernandez-Marcos¹ 

¹*Metabolic Syndrome Group (BIOPROMET), Madrid Institute for Advanced Studies (IMDEA) Food, E28049, Madrid, Spain*

²*Molecular Biology Center Severo Ochoa (CBMSO), Spanish National Research Council (CSIC), Madrid Autonoma University (UAM), Madrid, Spain*

³*Department of Basic Medical Sciences, Institute of Applied Molecular Medicine, School of Medicine, University Studies Center (CEU)-San Pablo University, Madrid, Spain*

⁴*Metabolism and Cell Signaling Laboratory, Spanish National Cancer Research Centre (CNIO), Madrid, Spain*

⁵*Flow Cytometry Unit, Biotechnology Programme, Spanish National Cancer Research Centre (CNIO), Madrid, Spain*

Correspondence

Pablo Jose Fernandez-Marcos, Metabolic Syndrome Group (BIOPROMET). Madrid Institute for Advanced Studies (IMDEA) Food, E28049, Madrid, Spain.

Email: pablojose.fernandez@imdea.org

ORCID

Andrés Pastor-Fernández  <https://orcid.org/0000-0002-8060-073X>

Manuel Montero Gómez de las Heras  <https://orcid.org/0000-0001-7447-694X>

Pablo Jose Fernandez-Marcos  <https://orcid.org/0000-0003-3515-4125>

REFERENCES

1. Barradas M, Plaza A, Colmenarejo G, Lázaro I, Costa-Machado LF, Martín-Hernández R, et al. Fatty acids homeostasis during fasting predicts protection from chemotherapy toxicity. *Nat Commun.* 2022;13(1):5677.
2. Pietrocola F, Pol J, Vacchelli E, Rao S, Enot DP, Baracco EE, et al. Caloric Restriction Mimetics Enhance Anticancer Immunosurveillance. *Cancer Cell.* 2016;30(1):147-60
3. Di Biase S, Lee C, Brandhorst S, Manes B, Buono R, Cheng CW, et al. Fasting-Mimicking Diet Reduces HO-1 to Promote T Cell-Mediated Tumor Cytotoxicity. *Cancer Cell.* 2016;30(1):136-46.
4. Ajona D, Ortiz-Espinosa S, Lozano T, Exposito F, Calvo A, Valencia K, et al. Short-term starvation reduces IGF-1 levels to sensitize lung tumors to PD-1 immune checkpoint blockade. *Nat Cancer.* 2020;1(1):75-85.
5. Hiramoto K, Homma T, Jikumaru M, Miyashita H, Sato EF, Inoue M. Fasting Differentially Modulates the Immunological System: Its Mechanism and Sex Difference. *J Clin Biochem Nutr.* 2008;43(2):75-81.
6. Jensen TL, Kiersgaard MK, Sørensen DB, Mikkelsen LF. Fasting of mice: a review. *Lab Anim.* 2013;47(4):225-40.
7. Chan JL, Heist K, DePaoli AM, Veldhuis JD, Mantzoros CS. The role of falling leptin levels in the neuroendocrine and metabolic adaptation to short-term starvation in healthy men. *Eur J Clin Invest.* 2003;111(9):1409.
8. Plaza A, Pastor-Fernández A, López-Aceituno JL, Barradas M, Pantoja C, Fernandez-Marcos PJ. p21 is necessary for the beneficial effects of fasting during chemotherapy. *Cancer Commun. (London, England).* 2023;43(1):164-68.
9. Vinay DS, Kwon BS. CD11c+CD8+ T cells: Two-faced adaptive immune regulators. *Cell Immunol.* 2010;264(1):18-22.
10. Vernieri C, Fuca G, Ligorio F, Huber V, Vingiani A, Iannelli F, et al. Fasting-mimicking diet is safe and reshapes metabolism and antitumor immunity in cancer patients. *Cancer Discov.* 2022;12(1):90-107.

SUPPORTING INFORMATION

Additional supporting information can be found online in the Supporting Information section at the end of this article.